

Article

Fixed-Time Coverage Control of Mobile Robot Networks Considering the Time Cost Metric

Qihai Sun ¹, Tianjun Liao ², Zhi-Wei Liu ¹, Ming Chi ^{1,*} and Dingxin He ¹

¹ School of Artificial Intelligence and Automation, Huazhong University of Science and Technology, Wuhan 430074, China

² Academy of Military Sciences, Beijing 100000, China

* Correspondence: chiming@hust.edu.cn

Abstract: In this work, we studied the area coverage control problem (ACCP) based on the time cost metric of a robot network with an input disturbance in a dynamic environment, which was modeled by a time-varying risk density function. A coverage control method based on the time cost metric was proposed. The area coverage task that considers the time cost consists of two phases: the robot network is driven to cover the task area with a time-optimal effect in the first phase; the second phase is when the accident occurs and the robot is driven to the accident site at maximum speed. Considering that there were movable objects in the task area, a time-varying risk density function was used to describe the risk degree at different locations in the task area. In the presence of the input disturbance, a robust controller was designed to drive each robot, with different maximum control input values, to the position that locally minimized the time cost metric function in a fixed time, and the conditions for maximum control input were obtained. Finally, simulation results and comparison result are presented in this paper.

Keywords: multi-robot network; dynamic environment coverage; time cost metric; fixed-time control



Citation: Sun, Q.; Liao, T.; Liu, Z.-W.; Chi, M.; He, D. Fixed-Time Coverage Control of Mobile Robot Networks Considering the Time Cost Metric. *Sensors* **2022**, *22*, 8938. <https://doi.org/10.3390/s22228938>

Academic Editor: Andrey V. Savkin

Received: 23 September 2022

Accepted: 17 November 2022

Published: 18 November 2022

Publisher's Note: MDPI stays neutral with regard to jurisdictional claims in published maps and institutional affiliations.



Copyright: © 2022 by the authors. Licensee MDPI, Basel, Switzerland. This article is an open access article distributed under the terms and conditions of the Creative Commons Attribution (CC BY) license (<https://creativecommons.org/licenses/by/4.0/>).

1. Introduction

Multi-robot cooperative control has drawn increasing attention from academics throughout the world due to the ongoing development of robotics technologies and related theories [1–4]. Robots need to be effectively controlled in various applications [5]. The ACCP is a crucial area of research in multi-robot cooperative control because it deals with how the robot network is distributed spatially within the area of interest so that it can be successfully observed or sensed [6–8]. The division of the task area into many sub-areas, with each robot solely covering its respective sub-area, is a key tactic for the area coverage of a multi-robot network. Researchers have frequently exploited the divide-and-conquer strategy to create area coverage control techniques, the most notable of which being Voronoi partitioning [9].

Based on the Voronoi partition method, some work has considered the ACCP in different environments and application scenarios. The authors of [10] proposed a cooperative area exploration strategy of the robot network based on the Voronoi partitioning approach. Based on the Voronoi partition method, the deployment of unmanned aerial vehicles (UAVs), while maintaining the connection between UAVs and base stations, was studied in [11]. Robots with different sensing abilities performed area coverage tasks in [12,13]. Coverage control was carried out for mobile robots with limited sensing or communication in distance [14–16]. An adaptive method was proposed to deploy sensor nodes to sense an area with unknown environmental density [17]. The non-parametric Gaussian statistical regression method to estimate density function online was used in [18].

Generally, the environmental density function, which describes the importance of each position in the task area, is time-invariant. However, in some applications, there may be some important movable objects in the task area, and their influence on the area

environment dynamically changes. Therefore, the environment density functions in some practical application scenarios are time-varying functions. Consider that there are movable objects in an ACCP, ref. [19] proposed a decentralized control law for the mobile robot network. Neutralization of pollutants in a area with mobile pollution sources was addressed in [20]. In the dynamic environment, the discrete coverage control problem was solved based on the k-means method in [21]. Considering unicycle model robots, the area coverage control of underactuated robots in dynamic environments was studied in [22,23].

The purpose of the above research about ACCPs is to minimize the sensing cost or maximize the monitoring probability. However, if the goal is to respond quickly to accidents in the area, the coverage control above will no longer be applicable, and the time cost should be used to measure the coverage effect. A few of scholars have paid attention to the time cost of coverage and have proposed some time-optimized coverage control (T-OCC) methods. Ru et al., considering both energy loss and moving time, ref. [24] solved the minimum cost coverage control problem by using a multi-objective optimization function. When there is a drift field, the ACCP considering time cost for the unicycle network was solved in [25]. For time-sensitive coverage tasks, ref. [26] solved the ACCP when the maximum velocity of each robot was different. The ACCP based on time cost is generally divided into two phases. The time cost is considered in the metric function of the coverage effect, and the robot network is driven to minimize the time cost metric function (TCMF) in the first phase. The second phase is when an accident occurs and the robot is driven to reach the accident site at maximum speed. However, in the current study of T-OCC [24–26], the first phase was achieved asymptotically, which did not ensure a quick response of the robot network.

Unlike other works that aimed to maximize the coverage monitoring probability or minimize the sensing cost in ACCP, the influence of the coverage time cost was considered, and the ACCP was solved with respect to the robot network in a dynamic environment. In addition, as opposed to the existing work related to the ACCP, a fixed-time robust controller was designed to drive each robot with a different maximum control input to minimize the TCMF, considering input disturbances, and the conditions that the control input should satisfy were analyzed. Finally, several simulation results were obtained, and the results of the comparison between the proposed control and the classical Lloyd algorithm [9,26] are presented in this paper.

This remainder of this paper is organized as follows. The kinematics of the robot and the generalized Voronoi partition method based on the shortest time principle are presented in Section 2. The coverage metric function with respect to time cost is given and analyzed in Section 3. The control law of time optimal coverage effect is presented in Section 4. Sections 5 and 6 present, respectively, the simulation results and conclusions.

2. Preliminaries

Mobile robots mainly include aerial aircraft [27,28], mobile cars on the road [29–31] and unmanned surface vessels on the water [32,33]. If we consider that N single integral model robots are used in a two-dimensional convex task area $Q \in R^2$, we define the robots' set \mathcal{V} ($\mathcal{V} = \{1, 2, \dots, N\}$), and the robots' kinematics are modeled as [29,34]

$$\dot{p} = \begin{bmatrix} \dot{x} \\ \dot{y} \end{bmatrix} = \begin{bmatrix} u_x \\ u_y \end{bmatrix} + \begin{bmatrix} d_x \\ d_y \end{bmatrix} = u + d, \quad (1)$$

where $p = [x, y]^T \in R^2$ is a robot's position in the earth-fixed frame, the control input is $u = [u_x, u_y]^T$ and the disturbance $d = [d_x, d_y]^T$ is bounded ($\|d(t)\| < \rho$). It is assumed that the maximum control inputs of each robot are different and bounded.

This paper considered coverage control with respect to the time cost metric. Inspired by Voronoi division [9,35], which is based on the principle of proximity as shown in Figure 1a, the task area Q was divided using the principle of shortest time, called the generalized Voronoi partition, as shown in Figure 1b:

$$V_i = \{q \in Q | t_{(p_i,q)} \leq t_{(p_j,q)}, \forall j \in \mathcal{V}\}, \quad (2)$$

where $t_{(p_i,q)} = \frac{\|p_i - q\|}{v_{i_max}}$ is the minimum time taken for the i -th robot to move from position p_i to position q ($q \in Q$) at the maximum speed v_{i_max} .

The risk degree in Q is described by a time-varying function $\psi(q, t)$,

$$\psi(q, t) = \phi(q) + \sum_{j=1}^M \phi_j(q, t),$$

where $\phi(q)$ represents the constant risk in the area and $\phi_j(q, t)$ ($j = 1, \dots, M$) is the contribution of the j -th movable object on the task area. This was different from most studies that have only considered the time-invariant risk $\phi(q)$ [7–9,12–18,24–26].

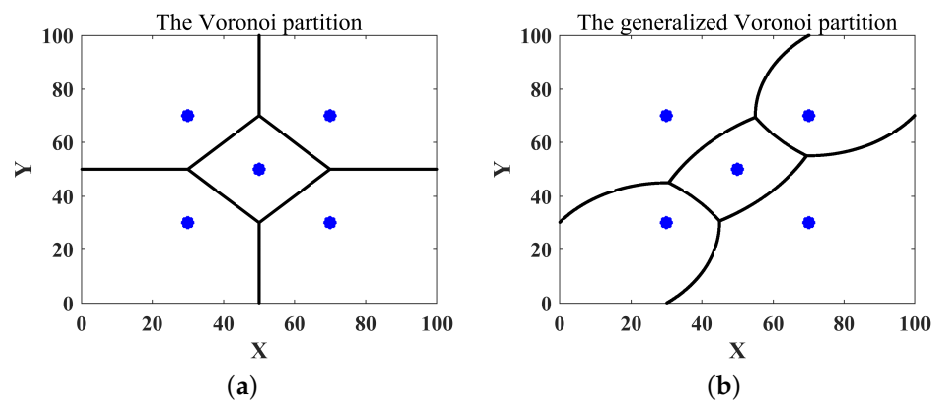


Figure 1. The Voronoi partition based on the proximity principle (a) and the generalized Voronoi partition based on the shortest time principle (b) (where the blue point “•” represents the position of the robot, and each robot had a different maximum speed v_{i_max} ($i \in \mathcal{V}$)).

3. Time Optimal Coverage Analysis

The purpose of this paper was to dynamically deploy the robot network in the task area to achieve the time optimal coverage effect, which was quantified by the TCMF

$$H_t(P, t) = \sum_{i=1}^N \int_{V_i} \left(t_{(p_i,q)} \right)^2 \psi(q, t) dq. \quad (3)$$

Lemma 1 (The Leibniz integral rule [36]). *The area V , which is smoothly dependent on position p , has a uniquely defined outer normal vector $n(q)$ anywhere on its boundary $\partial V(q)$. For the function*

$$\Omega = \int_{V(q)} h(p, q) dq,$$

one has

$$\frac{\partial \Omega}{\partial p} = \int_{V(q)} \frac{\partial h(p, q)}{\partial p} dq + \int_{\partial V(q)} h(p, q) n(q)^T \frac{\partial q}{\partial p} dq.$$

For the TCMF (3), one has

$$\begin{aligned}
 H_t(P, t) &= \int_{V_i} \left(t_{(p_i, q)} \right)^2 \psi(q, t) dq \\
 &+ \sum_{j \in \mathcal{N}_i} \int_{V_j} \left(t_{(p_i, q)} \right)^2 \psi(q, t) dq \\
 &+ \sum_{j \notin \{i\} \cup \mathcal{N}_i} \int_{V_j} \left(t_{(p_i, q)} \right)^2 \psi(q, t) dq,
 \end{aligned} \tag{4}$$

where \mathcal{N}_i is the neighbor set of the robot i , which is defined as the other robots that the Voronoi partitions have a common edge, V_i , with. The p_i partial derivative of $H_t(P, t)$ yields

$$\begin{aligned}
 \frac{\partial H_t(P, t)}{\partial p_i} &= \frac{\partial \left(\int_{V_i} \left(t_{(p_i, q)} \right)^2 \psi(q, t) dq \right)}{\partial p_i} \\
 &+ \frac{\partial \left(\sum_{j \in \mathcal{N}_i} \int_{V_j} \left(t_{(p_i, q)} \right)^2 \psi(q, t) dq \right)}{\partial p_i}.
 \end{aligned} \tag{5}$$

According to the Leibniz formula, one has the following:

$$\begin{aligned}
 \frac{\partial H_t(P, t)}{\partial p_i} &= \frac{2}{v_{i_max}^2} \int_{V_i} (p_i - q)^T \psi(q, t) dq \\
 &+ \sum_{j \in \mathcal{N}_i} \int_{\partial V_{i,j}} \left(\frac{\| p_i - q \|}{v_{i_max}} \right)^2 \psi(q, t) n_i(q)^T \frac{\partial q}{\partial p} dq \\
 &+ \sum_{j \in \mathcal{N}_i} \int_{\partial V_j} \left(\frac{\| p_j - q \|}{v_{j_max}} \right)^2 \psi(q, t) n_j(q)^T \frac{\partial q}{\partial p} dq,
 \end{aligned} \tag{6}$$

where $\partial V_{i,j}$ is the common edge of V_i and V_j and $n_i(q), n_j(q)$ are the outward normal vectors of V_i, V_j at the boundary $\partial V_{i,j}$, respectively, and one has

$$n_i(q) = -n_j(q). \tag{7}$$

Substituting (7) into Equation (6) yields

$$\begin{aligned}
 \frac{\partial H_t(P, t)}{\partial p_i} &= \frac{2}{v_{i_max}^2} \int_{V_i} (p_i - q)^T \psi(q, t) dq + \sum_{j \in \mathcal{N}_i} \int_{\partial V_{i,j}} \left(\frac{\| p_i - q \|}{v_{i_max}} \right)^2 \psi(q, t) n_i(q)^T \frac{\partial q}{\partial p} dq \\
 &- \sum_{j \in \mathcal{N}_i} \int_{\partial V_{i,j}} \left(\frac{\| p_j - q \|}{v_{j_max}} \right)^2 \psi(q, t) n_i(q)^T \frac{\partial q}{\partial p} dq \\
 &= \frac{2}{v_{i_max}^2} \int_{V_i} (p_i - q)^T \psi(q, t) dq \\
 &+ \sum_{j \in \mathcal{N}_i} \int_{\partial V_{i,j}} \left[\left(\frac{\| p_i - q \|}{v_{i_max}} \right)^2 - \left(\frac{\| p_j - q \|}{v_{j_max}} \right)^2 \right] \psi(q, t) n_i(q)^T \frac{\partial q}{\partial p} dq.
 \end{aligned} \tag{8}$$

Note that, when the point p is on the common edge $\partial V_{i,j}$, one has

$$t_{\min(p_i,q)}=t_{\min(p_j,q)} \Rightarrow \frac{\|p_i - q\|}{v_{i\text{-max}}} = \frac{\|p_j - q\|}{v_{j\text{-max}}}. \quad (9)$$

Substituting (9) into (8) yields

$$\begin{aligned} \frac{\partial H_t(P)}{\partial p_i} &= \frac{2}{v_{i\text{-max}}^2} \int_{V_i} (p_i - q)^T \psi(q, t) dq \\ &= \frac{2}{v_{i\text{-max}}^2} M_{V_i} (p_i - C_{V_i}), \end{aligned} \quad (10)$$

where

$$M_i = \int_{V_i} \psi(q, t) dq$$

is the mass of V_i , and

$$C_i = \begin{bmatrix} C_{xi} \\ C_{yi} \end{bmatrix} = \frac{\int_{V_i} q \psi(q, t) dq}{\int_{V_i} \psi(q, t) dq}$$

is the centroid of V_i .

Obviously, if the position p_i coincides with the centroid C_i , the p_i derivative of metric function $H_t(P, t)$ is zero. That is, the robot i achieves the optimal coverage effect of the partition V_i with the metric function $H_t(P, t)$. When each robot achieves the optimal coverage effect of its Voronoi partition, the robot network achieves the local optimal coverage effect of the task area Q . Next, the T-OCC of the robot network was designed to achieve a time-optimal coverage effect.

4. Fixed-Time Coverage Control

The above chapter analyzed and obtained the optimal position configuration of a robot network. Based on the sliding mode control method and the fixed-time stability theory, the fixed-time coverage controller was designed for a robot network. First, the controller forced states in the robot network to stabilize it on the sliding surfaces in a fixed time. Then, the position configuration of the robot network could track the optimal position configuration on the sliding surface in a fixed time. The control process is shown in Figure 2.

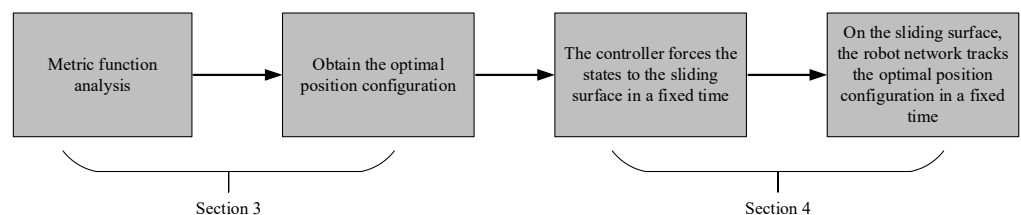


Figure 2. Fixed-time coverage control process of a mobile robot network with respect to the time cost metric.

Lemma 2 (Fixed-time stability theory [37–39]). Consider the system $\dot{x}(t) = f(x(t))$, if there is a function $V(x) : \mathbb{R}^N \rightarrow \mathbb{R}^N$ that is continuously positive definite and there are real numbers $k_1, k_2 > 0, q > 1, p \in (0, 1)$ that satisfy:

$$\dot{V}(x) \leq -(k_1(V(x))^q + k_2(V(x))^p), x \in \mathbb{R}^N \setminus \{0\},$$

then the system can stabilize to the origin in fixed time.

Define the position error as follows:

$$e_i = \begin{bmatrix} e_{xi} \\ e_{yi} \end{bmatrix} = \begin{bmatrix} x_i - C_{xi} \\ y_i - C_{yi} \end{bmatrix} (i \in \mathcal{V}).$$

Design the sliding surfaces as follows:

$$\begin{bmatrix} s_{xi} \\ s_{yi} \end{bmatrix} = \begin{bmatrix} x_i - g_{xi} \\ y_i - g_{yi} \end{bmatrix} (i \in \mathcal{V}). \quad (11)$$

The variables g_{xi} and g_{yi} are defined as follows:

$$\begin{aligned} \dot{g}_{xi} &= \dot{C}_{xi} - k_1 \|e_{xi}\|^{\alpha_1} \text{sgn}(e_{xi}) - k_2 \|e_{xi}\|^{\alpha_2} \text{sgn}(e_{xi}), \\ \dot{g}_{yi} &= \dot{C}_{yi} - k_3 \|e_{yi}\|^{\alpha_3} \text{sgn}(e_{yi}) - k_4 \|e_{yi}\|^{\alpha_4} \text{sgn}(e_{yi}), \end{aligned} \quad (12)$$

where k_1, k_2, k_3, k_4 are positive constant coefficients, $0 < \alpha_1, \alpha_3 < 1, \alpha_2, \alpha_4 > 1$ and \dot{C}_i is a bounded time derivative [40].

Considering the presence of the input disturbance, the fixed-time controller for the robot i can be designed as

$$u_i = \begin{bmatrix} u_{xi} \\ u_{yi} \end{bmatrix} = \begin{bmatrix} \dot{g}_{xi} - b_1 \|s_{xi}\|^{\beta_1} \text{sgn}(s_{xi}) \\ -b_2 \|s_{xi}\|^{\beta_2} \text{sgn}(s_{xi}) - \rho \cdot \text{sgn}(s_{xi}) \\ \dot{g}_{yi} - b_3 \|s_{yi}\|^{\beta_3} \text{sgn}(s_{yi}) \\ -b_4 \|s_{yi}\|^{\beta_4} \text{sgn}(s_{yi}) - \rho \cdot \text{sgn}(s_{yi}) \end{bmatrix}, \quad (13)$$

where the coefficients $b_1, b_2, b_3, b_4 > 0, -1 < \beta_1, \beta_3 < 0$ and $\beta_2, \beta_4 > 1$.

Let

$$u_{xi_max} = \max(\|u_{xi}(t)\|), u_{yi_max} = \max(\|u_{yi}(t)\|)$$

be the maximum values of the control input u_{xi}, u_{yi} , the main result is stated as follows.

Theorem 1. For the mobile robot network with dynamics (1), the controller (13) can drive the state of robot $i (i \in \mathcal{V})$ to reach the sliding surface (11) within the fixed time T_1 , and the time T_1 depends only on the controller parameters, not on the initial state of the robot i ,

$$T_1 = \frac{1}{2(b_1)^{\frac{2}{\beta_1+1}} (1 - \frac{\beta_1+1}{2})} + \frac{1}{2(b_2)^{-\frac{2}{\beta_2+1}} (\frac{\beta_2+1}{2} - 1)},$$

where the maximum values of the control inputs need to be

$$\begin{bmatrix} u_{xi_max} \\ u_{yi_max} \end{bmatrix} \geq \begin{bmatrix} \rho + \|\dot{g}_{xi}\| \\ \rho + \|\dot{g}_{xi}\| \end{bmatrix}.$$

Proof of Theorem 1. Define a Lyapunov function

$$V_1(s_{xi}) = \frac{1}{2} s_{xi} \cdot s_{xi}. \quad (14)$$

Taking the time derivative of $V_1(s_{xi})$ yields

$$\begin{aligned} \frac{V_1(s_{xi})}{dt} &= s_{xi} \cdot (\dot{x}_i - \dot{g}_{xi}) \\ &= s_{xi} \cdot (u_{xi} + d_{xi} - \dot{g}_{xi}) \\ &= s_{xi} \cdot (-b_1 \|s_{xi}\|^{\beta_1} \text{sgn}(s_{xi}) - b_2 \|s_{xi}\|^{\beta_2} \text{sgn}(s_{xi}) - \rho \cdot \text{sgn}(s_{xi}) + d_{xi}) \\ &= -b_1 \|s_{xi}\|^{\beta_1+1} - b_2 \|s_{xi}\|^{\beta_2+1} - (\rho \|s_{xi}\| - d_{xi} \cdot s_{xi}). \end{aligned} \quad (15)$$

Since the input disturbance $d_{xi}(t)$ is bounded ($\|d_i(t)\| < \rho$), it can be given that $d_{xi} \cdot s_{xi} < \rho \|s_{xi}\|$. For function (15), it gives

$$\begin{aligned} \frac{V_1(s_{xi})}{dt} &< -b_1 \|s_{xi}\|^{\beta_1+1} - b_2 \|s_{xi}\|^{\beta_2+1} - (\rho \|s_{xi}\| - \rho \|s_{xi}\|) \\ &< -b_1 \|s_{xi}\|^{\beta_1+1} - b_2 \|s_{xi}\|^{\beta_2+1} \\ &< -\{2(b_1)^{\frac{2}{\beta_1+1}} V_1(s_{xi})\}^{\frac{\beta_1+1}{2}} - \{2(b_2)^{-\frac{2}{\beta_2+1}} V_1(s_{xi})\}^{\frac{\beta_2+1}{2}}. \end{aligned} \quad (16)$$

According to the Lemma 2, for the time $t > T_1$,

$$T_1 = \frac{1}{2(b_1)^{\frac{2}{\beta_1+1}} (1 - \frac{\beta_1+1}{2})} + \frac{1}{2(b_2)^{-\frac{2}{\beta_2+1}} (\frac{\beta_2+1}{2} - 1)},$$

$s_{xi} = 0$ is implemented. Similarly, $s_{yi} = 0$ can be implemented within a fixed time.

Next, the lower bounds of the u_{xi_max}, u_{yi_max} are analyzed. When $t < T_1$, it has to satisfy

$$\begin{aligned} -u_{xi_max} &\leq \dot{g}_{xi} - b_1 \|s_{xi}\|^{\beta_1} \text{sgn}(s_{xi}) \\ &\quad - b_2 \|s_{xi}\|^{\beta_2} \text{sgn}(s_{xi}) - \rho \cdot \text{sgn}(s_{xi}) \\ &\leq u_{xi_max}, \end{aligned}$$

such that

$$\begin{aligned} -u_{xi_max} - \dot{g}_{xi} + \rho \cdot \text{sgn}(s_{xi}) &\leq \\ -b_1 \|s_{xi}\|^{\beta_1} \text{sgn}(s_{xi}) - b_2 \|s_{xi}\|^{\beta_2} \text{sgn}(s_{xi}) & \\ \leq u_{xi_max} - \dot{g}_{xi} + \rho \cdot \text{sgn}(s_{xi}). & \end{aligned}$$

When $s_{xi} > 0$, the maximum value u_{xi_max} needs to satisfy

$$-u_{xi_max} - \dot{g}_{xi} + \rho < 0,$$

which can be rewritten as

$$u_{xi_max} > -\dot{g}_{xi} + \rho.$$

When $s_{xi} < 0$, the maximum value u_{xi_max} needs to satisfy

$$u_{xi_max} - \dot{g}_{xi} + \rho \cdot \text{sgn}(s_{xi}) > 0,$$

which can be rewritten as

$$u_{xi_max} > \dot{g}_{xi} - \rho.$$

In conclusion, it gives

$$u_{xi_max} > \|\dot{g}_{xi}\| + \rho.$$

Similarly, the maximum value u_{yi_max} needs to satisfy

$$u_{yi_max} > \|\dot{g}_{yi}\| + \rho.$$

Hence, the maximum values of the control inputs need to be

$$\begin{bmatrix} u_{xi_max} \\ u_{yi_max} \end{bmatrix} \geq \begin{bmatrix} \rho + \|\dot{g}_{xi}\| \\ \rho + \|\dot{g}_{yi}\| \end{bmatrix}. \tag{17}$$

The above analysis proves that the controller (13) can force states in the robot network to stabilize on the sliding surfaces in a fixed time, and the lower bounds for the maximum values of the control inputs are given. □

Remark 1. It can be noted that the values of $\dot{g}_{xi}, \dot{g}_{yi}$ are related to \dot{C}_i and parameters k_1, k_2, k_3, k_4 . The smaller the values of k_1, k_2, k_3, k_4 , the closer the values of $\dot{g}_{xi}, \dot{g}_{yi}$ are to $\dot{C}_{xi}, \dot{C}_{yi}$. In addition, it can be noted that the larger the values of u_{xi_max}, u_{yi_max} , the larger the coefficients $b_1, b_2, b_3, b_4, \beta_2, \beta_4$ can be, the smaller the coefficients β_1, β_3 can be and the smaller T_1 can be.

Theorem 2. When the robot’s state reaches the sliding surface (11), the controller (13) can drive the position p_i of robot i ($i \in \mathcal{V}$), track the Voronoi centroid C_i within a fixed time T_2 and the time optimal coverage effect is achieved, where

$$T_2 = T_1 + \frac{1}{2(k_1)^{\frac{2}{\alpha_1+1}} (1 - \frac{\alpha_1+1}{2})} + \frac{1}{2(k_2)^{-\frac{2}{\alpha_2+1}} (\frac{\alpha_2+1}{2} - 1)}.$$

Proof of Theorem 2. Define a positive definite Lyapunov function

$$V_2(e_{xi}) = \frac{1}{2}(x_i - C_{xi}) \cdot (x_i - C_{xi}). \tag{18}$$

Taking the time derivative of $V_2(e_{xi})$ yields

$$\begin{aligned} \frac{V_2(e_{xi})}{dt} &= (x_i - C_{xi}) \cdot (\dot{x}_i - \dot{C}_{xi}) \\ &= (x_i - C_{xi}) \cdot (u_{xi} + d_{xi} - \dot{C}_{xi}). \end{aligned} \tag{19}$$

According to Theorem 1, when $t > T_1, s_{xi} = 0, s_{yi} = 0$ and $\dot{x} = \dot{g}_{xi}$ can be obtained. For the function (19), one has

$$\begin{aligned} \dot{V}_2(e_{xi}) &= e_{xi} \cdot (-k_1 \|e_{xi}\|^{\alpha_1} \text{sign}(e_{xi}) - k_2 \|e_{xi}\|^{\alpha_2} \text{sign}(e_{xi})) \\ &= -(k_1 \|e_{xi}\|^{\alpha_1+1} + k_2 \|e_{xi}\|^{\alpha_2+1}) \\ &= -(\{2(k_1)^{\frac{2}{\alpha_1+1}} \frac{1}{2} e_{xi}^2\}^{\frac{\alpha_1+1}{2}} + \{2(k_2)^{\frac{2}{\alpha_2+1}} \frac{1}{2} e_{xi}^2\}^{\frac{\alpha_2+1}{2}}) \\ &= -\{2(k_1)^{\frac{2}{\alpha_1+1}} V_2(e_{xi})\}^{\frac{\alpha_1+1}{2}} - \{2(k_2)^{\frac{2}{\alpha_2+1}} V_2(e_{xi})\}^{\frac{\alpha_2+1}{2}}. \end{aligned} \tag{20}$$

According to Lemma 2, the position error e_{xi} can be stabilized to 0 ($e_{xi} = 0$) within the fixed time T_2 , where

$$T_2 = T_1 + \frac{1}{2(k_1)^{\frac{2}{\alpha_1+1}} (1 - \frac{\alpha_1+1}{2})} + \frac{1}{2(k_2)^{-\frac{2}{\alpha_2+1}} (\frac{\alpha_2+1}{2} - 1)}.$$

The quantify u_{xi_max} needs to satisfy

$$\begin{aligned} -u_{xi_max} &\leq \dot{g}_{xi} - b_1 \|s_{xi}\|^{\beta_1} \text{sgn}(s_{xi}) \\ -b_2 \|s_{xi}\|^{\beta_2} \text{sgn}(s_{xi}) - \rho(\|s_{xi}\|^{\beta_1} + \|s_{xi}\|^{\beta_2}) \text{sgn}(s_{xi}) &\cdot \\ &\leq u_{xi_max}. \end{aligned}$$

When $t > T_1$, one has $s_{xi} = 0$, and

$$-b_1 \|s_{xi}\|^{\beta_1} \text{sgn}(s_{xi}) - b_2 \|s_{xi}\|^{\beta_2} \text{sgn}(s_{xi}) - \rho(\|s_{xi}\|^{\beta_1} + \|s_{xi}\|^{\beta_2}) \text{sgn}(s_{xi}) = 0.$$

Therefore, the quantity u_{xi_max} needs to satisfy

$$-u_{xi_max} \leq \dot{g}_{xi} \leq u_{xi_max}.$$

Substituting (12) gives

$$-u_{xi_max} \leq \dot{C}_{xi} - k_1 \|e_{xi}\|^{\alpha_1} \text{sgn}(e_{xi}) - k_2 \|e_{xi}\|^{\alpha_2} \text{sgn}(e_{xi}) \leq u_{xi_max},$$

since the parameters $k_1, k_2 (k_1, k_2 > 0)$ can be arbitrarily small positive numbers, such that

$$u_{xi_max} > \|\dot{C}_{xi}\|. \quad (21)$$

In Theorem 1, the lower bound of the control input u_{xi_max} is given in (17), which has already satisfied the condition (21). Similarly, $e_{yi} = 0$ can be obtained within a fixed time T_2 . Therefore, the robot network can achieve the optimal position configuration in a fixed time, and the time optimal coverage effect for the task area is achieved. \square

Remark 2. If the quantities u_{xi_max}, u_{yi_max} are large enough, the parameters $k_1, k_2, k_3, k_4, \alpha_2, \alpha_4$ can be designed for larger values and the parameters α_1, α_3 can be designed for smaller values. Then, the fixed time T_2 can be smaller, and the robot i ($i \in \mathcal{V}$) can track the Voronoi centroid faster.

5. Simulation Examples

Several simulation experiments were carried out to verify the proposed T-OCC method. Consider a $100 \text{ m} \times 100 \text{ m}$ convex 2-D area, the robot network composed of four robots with maximum control inputs of 8 m/s, 10 m/s, 12 m/s and 9 m/s performed the area coverage task cooperatively. There were two important movable objects in the task area, and their motion trajectory was as follows:

$$\begin{aligned} x_1 &= 30 - 10 \sin(t/15), \quad y_1 = 30 + 10 \cos(t/15), \\ x_2 &= 90 - 0.5t, \quad y_2 = 90 - 0.5t. \end{aligned}$$

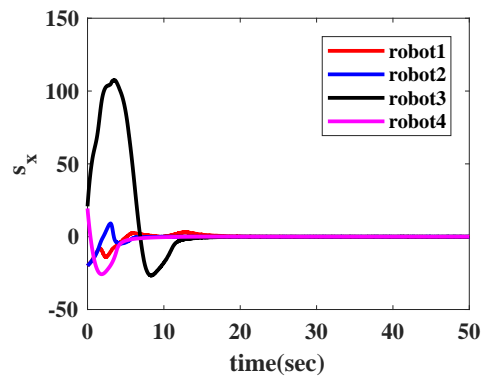
The contribution function $\phi_j(q, t)$ of the object j to the risk density is given as

$$\begin{aligned} \phi_1(q, t) &= 5e^{-\frac{\|q-m_1(t)\|^2}{200}}, \\ \phi_2(q, t) &= 3e^{-\frac{\|q-m_2(t)\|^2}{200}}, \end{aligned}$$

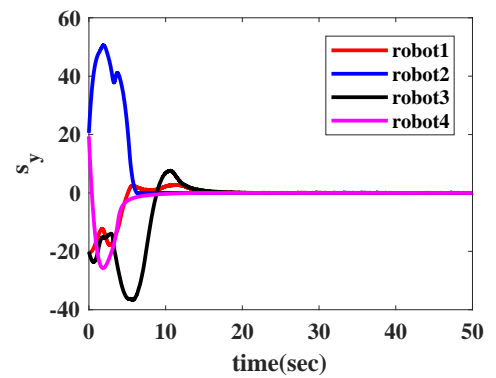
The input disturbance is given as $d_{xi} = 1 * \sin(t), d_{yi} = 1 * \cos(t)$. When the parameters of the designed controller were $k_1 = k_2 = k_3 = k_4 = 0.2, \alpha_1 = 0.8, \alpha_2 = 2, b_1 = b_2 = b_3 = b_4 = 0.2$ and $\beta_1 = 0.5, \beta_2 = 2$, the variation curves of states s_x, s_y are shown in Figure 3a,b, and the position errors e_x, e_y are shown in Figure 3c,d. It can be noted that the sliding mode surfaces s_x and s_y stabilized to 0 within 20 s, and the position errors e_x and e_y stabilized to 0 within 30 s.

We compared the proposed control algorithm (13) with the classical Lloyd algorithm [9,26]. The time evolution of the TCMF $H_t(P, t)$ is shown in Figure 3e. In Lloyd's algorithm, the control proportionality coefficient was set as 0.4, so that the two algorithms made the decrease rate of the metric function almost equal to the initial time. Figure 3f shows the comparison of the two algorithms. It could be noted that the control algorithm (13) could make the metric function smaller, therefore, the control algorithm had a better effect. The coverage evolution process of the robot network is shown in Figure 4. The distribution of the robot network was random at the initial time. Then, the robot network moved to the

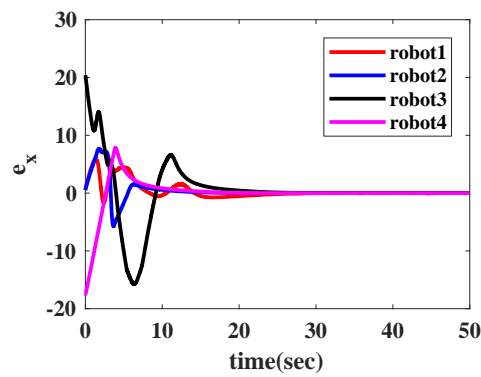
optimal position configuration and maintained the optimal coverage effect, despite several important objects in the area that were constantly moving.



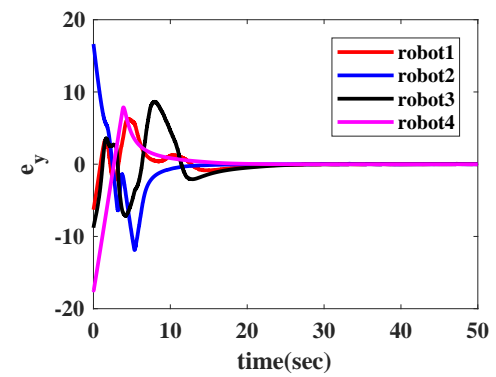
(a) The variation curve of the sliding mode surface s_x with respect to time t .



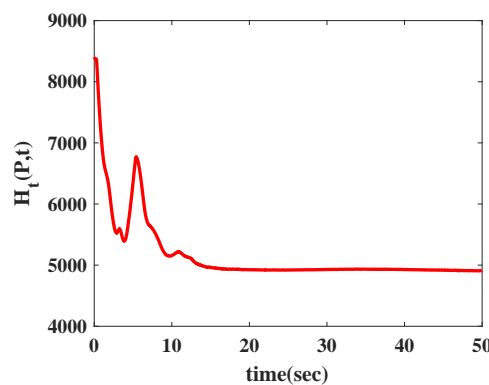
(b) The variation curve of the sliding mode surface s_y with respect to time t .



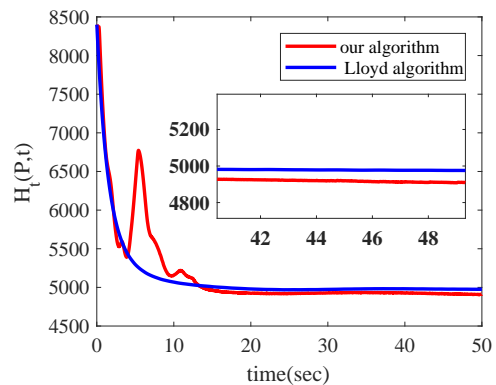
(c) The variation curve of the position error e_x with respect to time t .



(d) The variation curve of the position error e_y with respect to time t .



(e) The curve of the time cost metric function with respect to time t .



(f) Comparison of the coverage effect between our algorithm and the Lloyd algorithm.

Figure 3. The variation curves of s_x , s_y , e_x and e_y of the four robots with respect to time, the variation curves of metric function $H_t(P, t)$ and the comparison of optimization effects with the classic Lloyd algorithm.

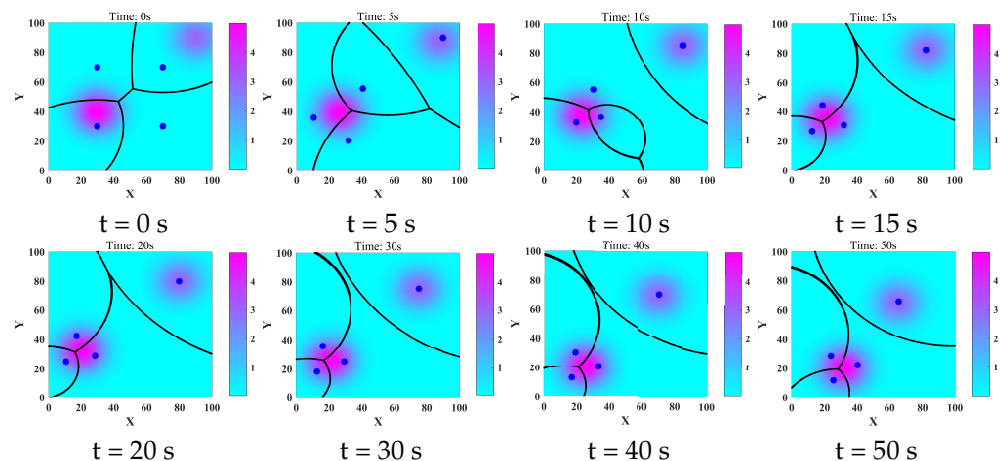


Figure 4. The coverage evolution process of the robot network to the task area, where the blue point “•” represents the position of the robot, and different colors in the area represent different risk degrees.

6. Conclusions

In this work, we studied the ACCP for a robot network in a dynamic environment considering the time cost. The most important findings are listed as follows:

1. When it is necessary to respond quickly to accidents, the coverage time cost is introduced to measure the coverage effect of the robot network on the task area;
2. Based on the TCMF, a fixed-time robust controller was designed to drive the robot network to achieve the minimum coverage time cost considering input disturbances;
3. The conditions that the maximum value of the control inputs should satisfy were obtained.

Collision avoidance in the coverage control will be the subject of future research.

Author Contributions: Conceptualization, Q.S. and Z.-W.L.; methodology, Q.S. and Z.-W.L.; software, Q.S. and T.L.; validation, Q.S., Z.-W.L. and M.C.; formal analysis, Q.S.; investigation, Q.S.; resources, Z.-W.L. and D.H.; data curation, Z.-W.L.; writing—original draft preparation, Q.S.; writing—review and editing, Z.-W.L.; visualization, Q.S. and T.L.; supervision, Z.-W.L.; project administration, Z.-W.L.; funding acquisition, D.H. All authors have read and agreed to the published version of the manuscript.

Funding: This research was funded by the National Natural Science Foundation of China under Grant 61973133, 62222205 and Grant 61972170.

Institutional Review Board Statement: Not applicable.

Informed Consent Statement: Not applicable.

Data Availability Statement: Not applicable.

Conflicts of Interest: The authors declare no conflict of interest.

References

1. Yang, D.; Li, X.; Song, S. Finite-time synchronization for delayed complex dynamical networks with synchronizing or desynchronizing impulses. *IEEE Trans. Neural Netw. Learn. Syst.* **2020**, *33*, 736–746. [[CrossRef](#)] [[PubMed](#)]
2. Ganesan, R.; Raajini, X.M.; Nayyar, A.; Sanjeevikumar, P.; Hossain, E.; Ertas, A.H. Bold: Bio-inspired optimized leader election for multiple drones. *Sensors* **2020**, *20*, 3134. [[CrossRef](#)] [[PubMed](#)]
3. Liu, Z.W.; Wen, G.; Yu, X.; Guan, Z.H.; Huang, T. Delayed impulsive control for consensus of multiagent systems with switching communication graphs. *IEEE Trans. Cybern.* **2019**, *50*, 3045–3055. [[CrossRef](#)] [[PubMed](#)]
4. Ge, M.F.; Liu, Z.W.; Wen, G.; Yu, X.; Huang, T. Hierarchical controller-estimator for coordination of networked Euler–Lagrange systems. *IEEE Trans. Cybern.* **2019**, *50*, 2450–2461. [[CrossRef](#)]
5. Astolfi, A.; Karagiannis, D.; Ortega, R. *Nonlinear and Adaptive Control with Applications*; Springer: Berlin/Heidelberg, Germany, 2008; Volume 187.

6. Cortés, J.; Egerstedt, M. Coordinated control of multi-robot systems: A survey. *SICE J. Control. Meas. Syst. Integr.* **2017**, *10*, 495–503.
7. Bai, Y.; Wang, Y.; Svinin, M.; Magid, E.; Sun, R. Adaptive multi-agent coverage control with obstacle avoidance. *IEEE Control Syst. Lett.* **2021**, *6*, 944–949. [[CrossRef](#)]
8. Arslan, Ö. Statistical coverage control of mobile sensor networks. *IEEE Trans. Robot.* **2019**, *35*, 889–908. [[CrossRef](#)]
9. Cortes, J.; Martinez, S.; Karatas, T.; Bullo, F. Coverage control for mobile sensing networks. *IEEE Trans. Robot. Autom.* **2004**, *20*, 243–255. [[CrossRef](#)]
10. Hu, J.; Niu, H.; Carrasco, J.; Lennox, B.; Arvin, F. Voronoi-based multi-robot autonomous exploration in unknown environments via deep reinforcement learning. *IEEE Trans. Veh. Technol.* **2020**, *69*, 14413–14423. [[CrossRef](#)]
11. Savkin, A.V.; Huang, H. Deployment of unmanned aerial vehicle base stations for optimal quality of coverage. *IEEE Wirel. Commun. Lett.* **2018**, *8*, 321–324. [[CrossRef](#)]
12. Laventall, K.; Cortés, J. Coverage control by multi-robot networks with limited-range anisotropic sensory. *Int. J. Control* **2009**, *82*, 1113–1121. [[CrossRef](#)]
13. Pierson, A.; Figueiredo, L.C.; Pimenta, L.C.; Schwager, M. Adapting to sensing and actuation variations in multi-robot coverage. *Int. J. Robot. Res.* **2017**, *36*, 337–354. [[CrossRef](#)]
14. Kantaros, Y.; Thanou, M.; Tzes, A. Distributed coverage control for concave areas by a heterogeneous robot–swarm with visibility sensing constraints. *Automatica* **2015**, *53*, 195–207. [[CrossRef](#)]
15. Santos, M.; Diaz-Mercado, Y.; Egerstedt, M. Coverage control for multirobot teams with heterogeneous sensing capabilities. *IEEE Robot. Autom. Lett.* **2018**, *3*, 919–925. [[CrossRef](#)]
16. Song, C.; Fan, Y. Coverage control for mobile sensor networks with limited communication ranges on a circle. *Automatica* **2018**, *92*, 155–161. [[CrossRef](#)]
17. Schwager, M.; Rus, D.; Slotine, J.J. Decentralized, adaptive coverage control for networked robots. *Int. J. Robot. Res.* **2009**, *28*, 357–375. [[CrossRef](#)]
18. Todescato, M.; Carron, A.; Carli, R.; Pillonetto, G.; Schenato, L. Multi-robots gaussian estimation and coverage control: From client–server to peer-to-peer architectures. *Automatica* **2017**, *80*, 284–294. [[CrossRef](#)]
19. Miah, S.; Panah, A.Y.; Fallah, M.M.H.; Spinello, D. Generalized non-autonomous metric optimization for area coverage problems with mobile autonomous agents. *Automatica* **2017**, *80*, 295–299. [[CrossRef](#)]
20. Luo, K.; Chi, M.; Chen, J.; Guan, Z.H.; Cai, C.X.; Zhang, D.X. Distributed coordination of multiple mobile actuators for pollution neutralization. *Neurocomputing* **2018**, *316*, 10–19. [[CrossRef](#)]
21. Yu, D.; Xu, H.; Chen, C.P.; Bai, W.; Wang, Z. Dynamic coverage control based on k-means. *IEEE Trans. Ind. Electron.* **2021**, *69*, 5333–5341. [[CrossRef](#)]
22. Sun, Q.; Liu, Z.W.; Chi, M.; Dou, Y.; He, D.; Qin, Y. Coverage control of unicycle multi-agent network in dynamic environment. *Math. Methods Appl. Sci.* **2021**. [[CrossRef](#)]
23. Sun, Q.; Chi, M.; Liu, Z.W.; He, D. Observer-Based coverage control of unicycle mobile robot network in dynamic environment. *J. Frankl. Inst.* **2022**. [[CrossRef](#)]
24. Ru, Y.; Martinez, S. Coverage control in constant flow environments based on a mixed energy–time metric. *Automatica* **2013**, *49*, 2632–2640. [[CrossRef](#)]
25. Zuo, L.; Chen, J.; Yan, W.; Shi, Y. Time-optimal coverage control for multiple unicycles in a drift field. *Inf. Sci.* **2016**, *373*, 571–580. [[CrossRef](#)]
26. Kim, S.; Santos, M.; Guerrero-Bonilla, L.; Yezzi, A.; Egerstedt, M. Coverage Control of Mobile Robots with Different Maximum Speeds for Time-Sensitive Applications. *IEEE Robot. Autom. Lett.* **2022**, *7*, 3001–3007. [[CrossRef](#)]
27. Ramírez-Rodríguez, J.; Tlatelpa-Osorio, Y.E.; Rodríguez-Cortés, H. Low level controller for quadrotors. In Proceedings of the 2021 International Conference on Unmanned Aircraft Systems (ICUAS), Athens, Greece, 15–18 June 2021; pp. 1155–1161.
28. Yayli, U.C.; Kimet, C.; Duru, A.; Cetir, O.; Torun, U.; Aydogan, A.C.; Padmanaban, S.; Ertas, A.H. Design optimization of a fixed wing aircraft. *Adv. Aircr. Spacecr. Sci.* **2017**, *4*, 65. [[CrossRef](#)]
29. Martinović, L.; Zečević, Ž.; Krstajić, B. Cooperative tracking control of single-integrator multi-agent systems with multiple leaders. *Eur. J. Control* **2022**, *63*, 232–239. [[CrossRef](#)]
30. Daya, F.J.; Sanjeevikumar, P.; Blaabjerg, F.; Wheeler, P.W.; Olorunfemi Ojo, J.; Ertas, A.H. Analysis of wavelet controller for robustness in electronic differential of electric vehicles: An investigation and numerical developments. *Electr. Power Compon. Syst.* **2016**, *44*, 763–773. [[CrossRef](#)]
31. Martínez, E.A.; Ríos, H.; Mera, M. Robust tracking control design for unicycle mobile robots with input saturation. *Control Eng. Pract.* **2021**, *107*, 104676. [[CrossRef](#)]
32. Qin, H.; Li, C.; Sun, Y.; Li, X.; Du, Y.; Deng, Z. Finite-time trajectory tracking control of unmanned surface vessel with error constraints and input saturations. *J. Frankl. Inst.* **2020**, *357*, 11472–11495. [[CrossRef](#)]
33. Lazarowska, A.; Żak, A. A Concept of Autonomous Multi-Agent Navigation System for Unmanned Surface Vessels. *Electronics* **2022**, *11*, 2853. [[CrossRef](#)]
34. Abdulghafoor, A.Z.; Bakolas, E. Two-Level Control of Multiagent Networks for Dynamic Coverage Problems. *IEEE Trans. Cybern.* **2021**. [[CrossRef](#)] [[PubMed](#)]
35. Erwig, M. The graph Voronoi diagram with applications. *Netw. Int. J.* **2000**, *36*, 156–163. [[CrossRef](#)]

36. Du, Q.; Faber, V.; Gunzburger, M. Centroidal Voronoi tessellations: Applications and algorithms. *SIAM Rev.* **1999**, *41*, 637–676. [[CrossRef](#)]
37. Polyakov, A. Nonlinear feedback design for fixed-time stabilization of linear control systems. *IEEE Trans. Autom. Control* **2011**, *57*, 2106–2110. [[CrossRef](#)]
38. Chen, Y.; Liu, Z.; Chen, C.L.P.; Zhang, Y. Adaptive Fuzzy Fixed-Time Control of Switched Systems: Mode-Dependent Power Integrator Method. *IEEE Trans. Syst. Man Cybern. Syst.* **2022**, *52*, 6998–7012. [[CrossRef](#)]
39. Zhuang, M.L.; Song, S.M. Fixed-time Coordinated Attitude Tracking Control for Spacecraft Formation Flying Considering Input Amplitude Constraint. *Int. J. Control. Autom. Syst.* **2022**, *20*, 2129–2147. [[CrossRef](#)]
40. Schwager, M.; Vitus, M.P.; Powers, S.; Rus, D.; Tomlin, C.J. Robust adaptive coverage control for robotic sensor networks. *IEEE Trans. Control Netw. Syst.* **2015**, *4*, 462–476. [[CrossRef](#)]